doi: 10.15407/ujpe62.01.0003

G.I. GAKH,[1,2] M.I. KONCHATNIJ,[1] N.P. MERENKOV [1,2]

[1] NSC "Kharkiv Institute of Physics and Technology", Nat. Acad. of Sci. of Ukraine
(1, Akademicheskaya Str., Kharkiv 61108, Ukraine; e-mail: konchatnij@kipt.kharkov.ua)
[2] Karazin Kharkiv National University
(4, Svoboda Sq., Kharkiv 61022,Ukraine)

MODEL-INDEPENDENT RADIATIVE CORRECTIONS TO ELASTIC PROTON-ELECTRON SCATTERING

PACS 12.20.-m,13.40.Gp

The model-independent QED radiative corrections to the differential cross-section of elastic scattering of a proton beam on electrons at rest have been calculated. The radiative corrections caused by the emission of virtual and soft real photons in the electron vertex and the vacuum polarization correction are taken into account. Numerical estimations of these corrections have been done.

K e y w o r d s: radiative corrections, elastic proton-electron scattering, inverse kinematics.

1. The polarized and unpolarized scatterings of electrons by protons has been widely studied, as it is considered the simpler way to access information on the proton structure. In the last time, the determination of the proton charge radius (PCR) with a help of muons leads to the so-called proton radius puzzle. A series of precise experiments with the purpose to determine PCR gave the results, which are in a strong disagreement with previous data. These results were obtained in the experiments on muonic hydrogen by the laser spectroscopy measurement of the μp (2S-2P) transition frequency [1, 2]. The latest result on PCR [2], $r = 0.84087(39)$ fm, obtained in this experiment is one order of magnitude more precise, but smaller by seven standard deviations compared to the average value $r = 0.8775(51)$ fm, which is recommended by the 2010-CODATA review [3]. This value was obtained by the hydrogen atom spectroscopy and electron-proton elastic scattering measurements. The latest experiments with electrons at Jlab [4] and MAMI [5] confirm this value. So, the results on PCR in the electron measurements do not agree with the results of the laser spectroscopy of muonic hydrogen.

While the corrections to the laser spectroscopy experiments seem well under control in the frame of QED and may be estimated with a precision better than 0.1%, the best precision, which has been achieved in case of the electron-proton elastic scattering, is of the order of few percent. Different sources of possible systematic errors in the muonic experiment have been discussed. However, no definite explanation of this difference has been given yet (see Ref. [6] and references therein).

The proton radius puzzle led to the appearance of a large number of papers trying to solve the problem. There are some approaches to do this. One of these approaches is to analyze more carefully the procedure of the PCR extraction from the *ep* scattering data. Thus, it has been suggested in Ref. [7] that PCR is actually measured in different frames (in the electron scattering and muonic hydrogen atoms) and that the Lorentz transformation of the form factors accounts properly for the discrepancy. The authors of Ref. [8] stated that the radius extraction with Taylor series expansions cannot be trusted to be reliable. A

fit function based on a conformal mapping was used in Ref. [9, 10]. The extracted value of the proton radius agrees with the one obtained from muonic hydrogen. In Ref. [11], the authors argued that the proton radius puzzle can be explained by truncating the electron scattering data to a low momentum transfer. But the authors of Ref. [12] showed that the procedure is inconsistent and violates the Fourier theorem.

To determine PCR, the authors of Ref. [13] reanalyzed the highest-accuracy electron-proton scattering data obtained by MAMI Collaboration [5] for the interval of the Q^2 values: $0.0038 \leq Q^2 \leq 1$ GeV^2. They found that these data are consistent with a much larger range of the PCR values than obtained by others. The obtained range for the PCR values (0.84–0.89 fm) is consistent with both methods (electron and muon ones) of the PCR determinations, and it was not strongly affected by the two-photon exchange effects. Lorenz *et al.* [14] have explicitly calculated two-photon exchange corrections to the electron-proton scattering including nucleon and Δ intermediate states, by using a phenomenological information on the vertices. They found that the dominating uncertainty is based on the choice of the nucleon form factors in the Born amplitude that enters the cross-section correction. The authors apply their two-photon exchange calculation to the MAMI cross-sections on the electron-proton scattering, where the kinematical conditions lead to the much smaller Δ contribution. Any curvature in the real form factor below the given data obviously leads to a bias due to the missing data. This might explain why PCR in conventional fits tends to come out large (for example, in the statistically sophisticated analysis [15]).

A comprehensive analysis of the electron-proton scattering data (high-statistics Mainz data set) has been done [16] to determine the proton electric and magnetic radii, by using model-independent constraints from the form factor analyticity. A wide-ranging study of the impact of potential systematic errors has been performed. Their analysis gives a value $r_E = 0.904(15)$ fm that is 4σ larger than the value obtained from the muon hydrogen spectroscopy. It was found that the charge radius puzzle persists. The circumstances, under which published muon hydrogen and electron-proton scattering data could be reconciled, are discussed. The review of the experimental and theoretical status of the nucleon form factors and the outlook for the future investigations is given in [17].

The another approach is the introduction of the beyond Standard Model physics. It was found [18] that a new scalar force carrier in the MeV mass range is not ruled out by the present data and accounts for the proton radius puzzle. The authors of Ref. [19] considered a combination of new vector and scalar particles which allowed them to explain the puzzle, while evading other constraints. The recent review summarizes the current state of the problem and gives an overview over upcoming experiments [20]. As stated there, in the next five years, a large number of experiments will shed some more light on this intriguing problem.

Formerly, a number of the experiments were done to measure the pion radius from the elastic scattering of negative pions on electrons in a liquid-hydrogen target. The first experiment was done at Serpukhov [21] with a pion beam energy of 50 GeV. Later, a few experiments were done at Fermilab with a pion beam energy of 100 GeV [22] and 250 GeV [23]. At that laboratory, the electromagnetic form factor of a negative kaon was measured by the direct scattering of 250-GeV kaons on the stationary electrons [24]. The typical values of radiative corrections (RCs) in this case are of the order of 7–10% [25].

Recently, we suggested that the proton elastic scattering on atomic electrons allows a precise measurement of PCR [26]. The main advantage of this proposal is that the inverse kinematics allows one to access, with a large cross-section, very small values of transferred momenta, up to four orders of magnitude smaller than the ones presently achieved. Some recent works have been devoted to the scattering of a proton projectile on an electron target (see [27] and references therein). But, for the analysis of the results of a possible experiment on the elastic p-e^- scattering, it is necessary to take RCs into account.

In this paper, we will calculate the model-independent QED RCs to the differential cross-section of the elastic scattering of the proton beam on electrons at rest. RCs, caused by the emission of virtual and soft real photons in the electron vertex and the vacuum polarization correction, are taken into account. Numerical estimations of these corrections have been done.

2. Let us consider the reaction

$$p\,(p_1) + e\,(k_1) \to p\,(p_2) + e\,(k_2), \qquad (1)$$

where the particle momenta are indicated in brackets, $q = k_1 - k_2 = p_2 - p_1$ is the four momentum of a virtual photon.

2.1. A general characteristic of all reactions of elastic and inelastic hadron scattering by atomic electrons (which can be considered at rest) is the small value of the transfer momentum squared, even for the relatively large energies of colliding particles. Let us give details of the order of magnitude and the dependence of the kinematic variables, as they are very specific for this reactions.

One can show that, for a given energy of the proton beam, the maximum value of the four momentum transfer squared in the scattering on the electron at rest is

$$(Q^2)_{\max} = \frac{4m^2\mathbf{p}^2}{M^2 + 2mE + m^2}, \tag{2}$$

where $m(M)$ is the electron (proton) mass, $Q^2 = -q^2$, $E(\mathbf{p})$ is the energy (momentum) of the proton beam. Being proportional to the electron mass squared, the four momentum transfer squared is restricted to very small values, where the proton can be considered point-like.

The four momentum transfer squared is expressed as a function of the energy of the scattered electron, ϵ_2, as $q^2 = (k_1 - k_2)^2 = 2m(m - \epsilon_2)$, and

$$\epsilon_2 = m\frac{(E+m)^2 + \mathbf{p}^2\cos^2\theta_e}{(E+m)^2 - \mathbf{p}^2\cos^2\theta_e}, \tag{3}$$

where θ_e is the angle between the proton beam and the scattered electron momenta.

From the energy and momentum conservation, one finds the following relation between the angle and the energy of the scattered electron:

$$\cos\theta_e = \frac{(E+m)(\epsilon_2 - m)}{|\mathbf{p}|\sqrt{(\epsilon_2^2 - m^2)}}, \tag{4}$$

which shows that $\cos\theta_e \geq 0$ (the electron can never be scattered backward). One can see from Eq. (3) that the available kinematical region is reduced to small values of ϵ_2:

$$\epsilon_{2,\max} = m\frac{2E(E+m) + m^2 - M^2}{M^2 + 2mE + m^2}, \tag{5}$$

which is proportional to the electron mass. From the momentum conservation, one can find the following relation between the energy E_2 and the angle θ_p of the scattered proton:

$$E_2^{\pm} = \frac{(E+m)(M^2+mE) \pm M\mathbf{p}^2\cos\theta_p\sqrt{\frac{m^2}{M^2} - \sin^2\theta_p}}{(E+m)^2 - \mathbf{p}^2\cos^2\theta_p}, \tag{6}$$

which shows that two values of the proton energy can be for one proton angle. The two solutions coincide, when the angle between the initial and final hadrons takes its maximum value, which is determined by the ratio of the electron and scattered hadron masses, $\sin\theta_{h,\max} = m/M$. One concludes that the hadrons are scattered on atomic electrons at very small angles, and that the larger the hadron mass, the smaller is the available angular range for the scattered hadron.

2.2. In the one-photon exchange (Born) approximation, the matrix element $\mathcal{M}^{(B)}$ of reaction (1) can be written as

$$\mathcal{M}^{(B)} = \frac{e^2}{q^2} j_\mu J_\mu, \tag{7}$$

where $j_\mu(J_\mu)$ is the leptonic (hadronic) electromagnetic current:

$$\begin{aligned} &j_\mu = \bar{u}(k_2)\gamma_\mu u(k_1), \\ &J_\mu = \bar{u}(p_2)\Big[F_1(q^2)\gamma_\mu - \frac{1}{2M}F_2(q^2)\sigma_{\mu\nu}q_\nu\Big]\times \\ &\times u(p_1) = \bar{u}(p_2)\left[G_M(q^2)\gamma_\mu - F_2(q^2)P_\mu\right]u(p_1), \end{aligned} \tag{8}$$

where $F_1(q^2)$ and $F_2(q^2)$ are the Dirac and Pauli proton electromagnetic form factors, $G_M(q^2) = F_1(q^2) + F_2(q^2)$ is the Sachs proton magnetic form factor, and $P_\mu = (p_1 + p_2)_\mu/(2M)$.

The matrix element squared is written as

$$\begin{aligned} &|\mathcal{M}^{(B)}|^2 = 16\pi^2\frac{\alpha^2}{q^4}L_{\mu\nu}W_{\mu\nu}, \\ &L_{\mu\nu} = j_\mu j_\nu^*,\ W_{\mu\nu} = J_\mu J_\nu^*, \end{aligned} \tag{9}$$

where $\alpha = 1/137$ is the electromagnetic fine structure constant. The leptonic tensor for unpolarized initial and final electrons (averaging over the initial electron spin) has the form

$$L_{\mu\nu} = q^2 g_{\mu\nu} + 2(k_{1\mu}k_{2\nu} + k_{1\nu}k_{2\mu}). \tag{10}$$

The hadronic tensor $W_{\mu\nu}$ for unpolarized initial and final protons can be written in the standard form in terms of two unpolarized structure functions:

$$W_{\mu\nu} = \Big(-g_{\mu\nu} + \frac{q_\mu q_\nu}{q^2}\Big) W_1\left(q^2\right) + P_\mu P_\nu W_2\left(q^2\right). \quad (11)$$

Averaging over the initial proton spin, the structure functions W_i, $i = 1, 2$, are expressed in terms of the nucleon electromagnetic form factors:

$$\begin{aligned} W_1\left(q^2\right) &= -q^2 G_M^2\left(q^2\right), \\ W_2\left(q^2\right) &= 4M^2 \frac{G_E^2\left(q^2\right) + \tau G_M^2\left(q^2\right)}{1+\tau}, \end{aligned} \quad (12)$$

where $G_E(q^2) = F_1(q^2) - \tau F_2(q^2)$ is the proton electric form factor, and $\tau = -q^2/4M^2$.

The expression for the differential cross-section, as a function of the recoil-electron energy ϵ_2, for the unpolarized proton-electron scattering can be written as

$$\begin{aligned} \frac{d\sigma^{(B)}}{d\varepsilon_2} &= \frac{\pi\alpha^2}{m\mathbf{p}^2}\frac{\mathcal{D}}{q^4}, \\ \mathcal{D} &= q^2\left(q^2+2m^2\right)G_M^2\left(q^2\right) + 2\Bigg[q^2M^2 + \\ &+ \frac{1}{1+\tau}\left(2mE + \frac{q^2}{2}\right)^2\Bigg]\Big[G_E^2\left(q^2\right) + \tau G_M^2\left(q^2\right)\Big]. \end{aligned} \quad (13)$$

This expression is valid in the one-photon exchange (Born) approximation in the reference system, where the target electron is at rest.

The differential cross-section, as a function of the variable q^2, is

$$\frac{d\sigma^{(B)}}{dq^2} = \frac{\pi\alpha^2}{2m^2\mathbf{p}^2}\frac{\mathcal{D}}{q^4}. \quad (14)$$

At last, the differential cross-section over the scattered-electron solid angle has the following expression:

$$\frac{d\sigma^{(B)}}{d\Omega_e} = \frac{\alpha^2}{8m^4|\mathbf{p}|}\left(1 - \frac{4m^2}{q^2}\right)^{3/2}\frac{D}{E+m}. \quad (15)$$

3. Let us consider the model-independent QED RCs which are caused by emission of the virtual and real soft photons in the electron vertex and the vacuum polarization.

3.1. In this section we calculate the contribution to RCs of the soft photon emission, when the photons are emitted by the initial and final electrons

$$p(p_1) + e(k_1) \to p(p_2) + e(k_2) + \gamma(k). \quad (16)$$

The matrix element in this case (photon is emitted from the electron vertex) is given by

$$\mathcal{M}^{(\gamma)} = \frac{1}{q^2}(4\pi\alpha)^{3/2} j_\mu^{(\gamma)} J_\mu, \quad (17)$$

where the electron current corresponding to the photon emission is

$$\begin{aligned} j_\mu^{(\gamma)} &= \bar{u}(k_2)\Bigg[\frac{1}{d_1}\gamma_\mu(\hat{k}_1 - \hat{k} + m)\gamma_\rho + \\ &+ \frac{1}{d_2}\gamma_\rho(\hat{k}_2 + \hat{k} + m)\gamma_\mu\Bigg]u(k_1)A_\rho^*, \end{aligned} \quad (18)$$

where A_ρ^* is the polarization vector of the emitted photon, and $d_1 = -2k\cdot k_1$, $d_2 = 2k\cdot k_2$.

The differential cross-section of reaction (17) can be written as

$$\begin{aligned} d\sigma^{(\gamma)} &= \frac{(2\pi)^{-5}}{32m|\mathbf{p}|}|\mathcal{M}^{(\gamma)}|^2 \times \\ &\times \frac{d^3\mathbf{k}_2}{\epsilon_2}\frac{d^3\mathbf{p}_2}{E_2}\frac{d^3\mathbf{k}}{\omega}\delta^4(k_1 + p_1 - k_2 - p_2 - k). \end{aligned} \quad (19)$$

It is necessary to integrate over the photon phase space. Since the photons are assumed soft, the integration over the photon energy is restricted to $|\mathbf{k}| \leq \leq \Delta E$. The quantity ΔE is determined by particular experimental conditions, and it is assumed that ΔE is sufficiently small in order to neglect the momentum k in the δ function and in the numerators of the matrix element $\mathcal{M}^{(\gamma)}$. In order to avoid the infrared divergence, which occurs in the soft photon cross-section, we have assumed a small photon mass λ.

In the soft photon approximation, the matrix element (17) is

$$\mathcal{M}^{(\mathrm{soft})} = \sqrt{4\pi\alpha}\left(\frac{k_2\cdot A^*}{k\cdot k_2} - \frac{k_1\cdot A^*}{k\cdot k_1}\right)\mathcal{M}^{(B)}. \quad (20)$$

The differential cross-section integrated over the soft photon phase space can be written as

$$d\sigma^{(\mathrm{soft})} = \delta_s d\sigma^{(B)}, \quad (21)$$

where RC due to the soft photon emission is

$$\delta_s = -\frac{\alpha}{4\pi^2}\int\limits_{\lambda}^{\Delta E} d\omega\left\{\sqrt{\omega^2-\lambda^2}\times\right.$$
$$\left.\times\int d\Omega_k\left[\frac{m^2}{(k\cdot k_1)^2}+\frac{m^2}{(k\cdot k_2)^2}-2\frac{k_1\cdot k_2}{k\cdot k_1 k\cdot k_2}\right]\right\}. \quad (22)$$

Using the results of work [28], we can do the integration, and the expression for δ_s is as follows:

$$\delta_s = \frac{\alpha}{\pi}\left\{1-2\ln\frac{2\Delta E}{\lambda}+\frac{\varepsilon_2}{k_2}\left[\ln\frac{\varepsilon_2+k_2}{m}\times\right.\right.$$
$$\times\left(1+2\ln\frac{2\Delta E}{\lambda}+\ln\frac{\varepsilon_2+k_2}{m}+2\ln\frac{m}{2k_2}\right)-$$
$$\left.\left.-\frac{\pi^2}{6}+\mathrm{Sp}\left(\frac{\varepsilon_2-k_2}{\varepsilon_2+k_2}\right)\right]\right\}, \quad (23)$$

where $\mathrm{Sp}(x)$ is the Spence (dilogarithm) function defined as

$$\mathrm{Sp}(x) = -\int\limits_0^x \frac{\ln(1-t)}{t}dt.$$

In the limiting case $Q^2 = 2m(\varepsilon_2 - m) \ll m^2$, the soft photon factor reads

$$\delta_s = \frac{\alpha}{\pi}\frac{Q^2}{m^2}\left[\frac{19}{9}-\frac{8}{3}\ln 2+\frac{4}{3}\ln\frac{m^2}{Q^2}+\frac{2}{3}\ln\frac{2\Delta E}{\lambda}\right],$$

where as at $Q^2 \gg m^2$ we have

$$\delta_s = \frac{\alpha}{\pi}\left[1-\frac{\pi^2}{6}+\ln\frac{Q^2}{m^2}-\ln^2\frac{Q^2}{m^2}+2\ln\frac{2\Delta E}{\lambda}\times\right.$$
$$\left.\times\left(\ln\frac{Q^2}{m^2}-1\right)+\frac{m^2}{Q^2}\left(2-4\ln\frac{Q^2}{m^2}+4\ln\frac{2\Delta E}{\lambda}\right)\right].$$

3.2. In this subsection, we calculate the contribution of the virtual photon emission in the electron vertex to RCs (the electron vertex correction) and the vacuum polarization term. The matrix element corresponding to this process can be written as

$$\mathcal{M}^{(\mathrm{virt})} = \frac{1}{q^2}4\pi\alpha J_\mu \bar{u}(k_2)\Lambda_\mu(k_1,k_2)u(k_1), \quad (24)$$

where we introduce

$$\Lambda_\mu(k_1,k_2) =$$
$$= \frac{2i\alpha}{(2\pi)^3}\int\frac{d^4k}{k^2-\lambda^2}\frac{\hat{O}_\mu}{(k^2-2k\cdot k_1)(k^2-2k\cdot k_2)}, \quad (25)$$

and the matrix $\hat{O}_\mu$ is

$$\hat{O}_\mu = 4k_1\cdot k_2\gamma_\mu - 2\left(\hat{k}_1\hat{k}\gamma_\mu+\gamma_\mu\hat{k}\hat{k}_2\right)-2\hat{k}\gamma_\mu\hat{k}. \quad (26)$$

The integration over the virtual-photon four-momentum k leads to the following expression for the function $\Lambda_\mu(k_1,k_2)$:

$$\Lambda_\mu(k_1,k_2) = \frac{\alpha}{4\pi}\left\{\left[\ln\frac{\Lambda^2}{m^2}+\frac{1}{2}+\int\limits_0^1\frac{dx}{P_x^2}\times\right.\right.$$
$$\left.\times\left(4m^2-\frac{3}{2}q^2+\left(q^2-2m^2\right)\left(\ln\frac{P_x^2}{m^2}+\ln\frac{m^2}{\lambda^2}\right)\right)\right]\gamma_\mu+$$
$$\left.+m\int\limits_0^1\frac{dx}{P_x^2}\sigma_{\mu\nu}q_\nu\right\}, \quad (27)$$

where $P_x^2 = m^2 - x(1-x)q^2$, and Λ is the parameter, which cuts the region of infinite momenta of the virtual photon. Thus, we avoid the ultraviolet divergence. The regularized vertex function can be obtained by the subtraction of the contribution

$$\Lambda_\mu(k_1,k_1) = \frac{\alpha}{4\pi}\gamma_\mu\left[\ln\frac{\Lambda^2}{m^2}+\frac{9}{2}-2\ln\frac{m^2}{\lambda^2}\right]$$

from expression (27). As a result, we have

$$\Lambda_\mu^R(k_1,k_2) = \Lambda_\mu(k_1,k_2)-\Lambda_\mu(k_1,k_1) =$$
$$= \frac{\alpha}{4\pi}(A\gamma_\mu+B\sigma_{\mu\nu}q_\nu), \quad (28)$$
$$A = -4+2\ln\frac{m^2}{\lambda^2}+\int\limits_0^1\frac{dx}{P_x^2}\left\{4m^2-\frac{3}{2}q^2+\right.$$
$$\left.+\left(q^2-2m^2\right)\left[\ln\frac{P_x^2}{m^2}+\ln\frac{m^2}{\lambda^2}\right]\right\},\ B = m\int\limits_0^1\frac{dx}{P_x^2}. \quad (29)$$

Because we calculate RC of the order of α in comparison with the Born term, it is sufficient to calculate the interference of the Born matrix element with $\mathcal{M}^{(\mathrm{virt})}$:

$$|\mathcal{M}|^2 = |\mathcal{M}^{(B)}|^2 + 2\mathrm{Re}[\mathcal{M}^{(\mathrm{virt})}\mathcal{M}^{(B*)}] =$$
$$= (1+\delta_1+\delta_2)|\mathcal{M}^{(B)}|^2, \quad (30)$$

where the term δ_1 is due to a modification of the γ_μ term in the electron vertex, and the term δ_2 is

caused by the appearance of the $\sigma_{\mu\nu}q_\nu$ structure in the electron vertex.

The integration over the variable x in expression (29) gives the following results for RCs caused by the emission of a virtual photon in the electron vertex

$$\delta_1 = \frac{\alpha}{\pi}\Bigg\{-2+2\ln\frac{m}{\lambda}\left[1-\frac{\varepsilon_2}{k_2}\ln\left(\frac{\varepsilon_2+k_2}{m}\right)\right]+$$
$$+\frac{m+3\varepsilon_2}{2k_2}\ln\left(\frac{\varepsilon_2+k_2}{m}\right)-\frac{1}{2}\frac{\varepsilon_2}{k_2}\times$$
$$\times\ln\left(\frac{-q^2}{m^2}\right)\ln\left(\frac{\varepsilon_2+k_2}{m}\right)+$$
$$+\frac{\varepsilon_2}{k_2}\Bigg[-\ln\left(\frac{m+\varepsilon_2}{k_2}\right)\ln\left(\frac{\varepsilon_2+k_2}{m}\right)+$$
$$+\mathrm{Sp}\left(\frac{\varepsilon_2+k_2+m}{2(m+\varepsilon_2)}\right)-\mathrm{Sp}\left(\frac{\varepsilon_2-k_2+m}{2(m+\varepsilon_2)}\right)\Bigg]\Bigg\},$$
$$\delta_2 = 4\frac{\alpha}{\pi}\frac{mM^2q^2}{k_2D}\ln\left(\frac{\varepsilon_2+k_2}{m}\right)(G_E^2-2\tau G_M^2). \qquad (31)$$

The limiting cases for δ_1 reads

$$\delta_1 = \frac{\alpha}{\pi}\frac{Q^2}{m^2}\left(\frac{1}{4}-\frac{2}{3}\ln\frac{m}{\lambda}\right),$$
$$\delta_1 = \frac{\alpha}{\pi}\Bigg[-2+\frac{\pi^2}{6}+\frac{3}{2}\ln\frac{Q^2}{m^2}-\frac{1}{2}\ln^2\frac{Q^2}{m^2}+$$
$$+2\ln\frac{m}{\lambda}\left(1-\ln\frac{Q^2}{m^2}\right)+\frac{m^2}{Q^2}\left(1-3\ln\frac{Q^2}{m^2}-4\ln\frac{m}{\lambda}\right)\Bigg],$$

at $Q^2 \ll m^2$ and $Q^2 \gg m^2$, respectively. RC due to the vacuum polarization can be written as (the electron loop has been taken into account)

$$\delta^{(\mathrm{vac})} = \frac{2\alpha}{3\pi}\Bigg\{-\frac{5}{3}+4\frac{m^2}{Q^2}+$$
$$+\left(1-2\frac{m^2}{Q^2}\right)\sqrt{1+4\frac{m^2}{Q^2}}\ln\frac{\sqrt{1+4\frac{m^2}{Q^2}}+1}{\sqrt{1+4\frac{m^2}{Q^2}}-1}\Bigg\}. \qquad (32)$$

For small and large values of the Q^2 variable, we have

$$\delta^{(\mathrm{vac})} = \frac{2\alpha}{15\pi}\frac{Q^2}{m^2},\ Q^2 \ll m^2;$$
$$\delta^{(\mathrm{vac})} = \frac{2\alpha}{3\pi}\left[-\frac{5}{3}+\ln\frac{Q^2}{m^2}\right],\ Q^2 \gg m^2.$$

Taking RCs given by Eqs. (23), (31), (32) into account, we obtain the following expression for the differential cross-section including RC in the considered approximation:

$$d\sigma^{(\mathrm{RC})} = (1+\delta_0+\bar{\delta}+\delta^{(\mathrm{vac})})d\sigma^{(B)}, \qquad (33)$$

where RCs δ_0 and $\bar{\delta}$ are given by

$$\delta_0 = \frac{2\alpha}{\pi}\ln\frac{\Delta E}{m}\left[\frac{\varepsilon_2}{k_2}\ln\left(\frac{\varepsilon_2+k_2}{m}\right)-1\right],$$
$$\bar{\delta} = \frac{\alpha}{\pi}\Bigg\{-1-2\ln 2+\frac{\varepsilon_2}{k_2}\Bigg[\ln\left(\frac{\varepsilon_2+k_2}{m}\right)\times$$
$$\times\left(1+\ln\left(\frac{\varepsilon_2+k_2}{m}\right)+2\ln\left(\frac{m}{k_2}\right)+\frac{m+3\varepsilon_2}{2\varepsilon_2}-\right.$$
$$\left.-\ln\left(\frac{\varepsilon_2+m}{k_2}\right)-\frac{1}{2}\ln\left(\frac{Q^2}{m^2}\right)\right)+$$
$$+4m\frac{M^2q^2}{\varepsilon_2 D}\ln\left(\frac{\varepsilon_2+k_2}{m}\right)(G_E^2-2\tau G_M^2)-\frac{\pi^2}{6}+$$
$$+\mathrm{Sp}\left(\frac{\varepsilon_2-k_2}{\varepsilon_2+k_2}\right)+\mathrm{Sp}\left(\frac{\varepsilon_2+k_2+m}{2(\varepsilon_2+m)}\right)-$$
$$-\mathrm{Sp}\left(\frac{\varepsilon_2-k_2+m}{2(\varepsilon_2+m)}\right)\Bigg]\Bigg\}. \qquad (34)$$

We separate the contribution δ_0, since it can be summed up in all orders of perturbation theory, by using the exponential form of the electron structure functions [29]. To do this, it is sufficient to keep only the exponential contributions to the electron structure functions. The final result can be obtained by the substitution of the term $(1+\delta_0)$ by the following term:

$$\frac{\beta}{2}\left(\frac{\Delta E}{m}\right)^\beta\int\limits_0^1 x^{\frac{\beta}{2}-1}(1-x)^{\frac{\beta}{2}}dx,$$
$$\beta = \frac{2\alpha}{\pi}\left[\frac{\varepsilon_2}{k_2}\ln\left(\frac{\varepsilon_2+k_2}{m}\right)-1\right]. \qquad (35)$$

4. Since Q^2 is very small in this reaction as compared with the proton mass squared, we use the Taylor series expansion for the proton charge form factor:

$$G_E(q^2) = 1+\frac{1}{6}q^2\langle r^2\rangle+O(q^2), \qquad (36)$$

where $\langle r^2\rangle$ is the mean-square radius of proton's electromagnetic charge distribution. As is seen from Eq. (13), the contribution of the magnetic form factor is suppressed by the factor q^2/M^2 compared with the charge form factor.

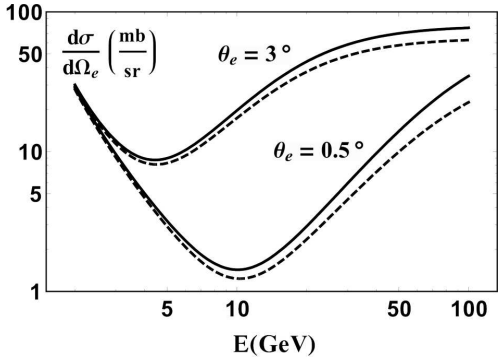

Fig. 1. Differential cross-section as a function of the proton-beam energy E for different angles θ_e without (solid line) and with (dashed line) regard for RC calculated with PCR extracted from the electron experiment

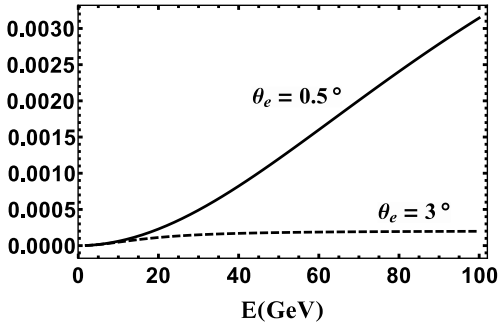

Fig. 2. Quantity (1-R) as a function of the proton-beam energy E for different angles θ_e. Here, $R = d\sigma_e/d\sigma_\mu$, where subscript $e(\mu)$ means that the differential cross-section is calculated with PCR determined from the electron (muon) experiments

In our calculations, we want to ensure the accuracy, which allows us to distinguish two values of PCR. For numerical results in this work, at very small values of Q^2, it is sufficient to use the static value of the form factor $G_M(q^2)$: $G_M(0) = 2.793$. For G_E^2, we use $G_E^2 = 1 + \frac{1}{3}\, q^2\, \langle r^2 \rangle$.

However, in other kinematical regions, it is necessary to use the more exact formula for the electric and magnetic form factors at least for the Born cross-section. For example, at $E = 100$ GeV, such region includes the recoil electron energies $\epsilon_2 \geq 5$ GeV. If we have to include the terms of the order of q^4 in the cross-section, it is necessary to use the following expressions for G_E and G_M:

$$G_E(q^2) = 1 + \frac{1}{6} q^2 \langle r^2 \rangle + \frac{1}{120} q^4 \langle r^4 \rangle,$$

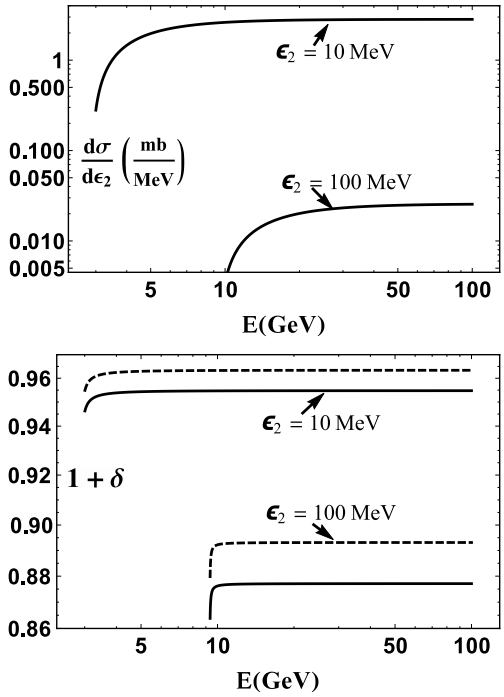

Fig. 3. Differential cross-section as a function of the proton-beam energy E for different recoil-electron energies ε_2 (upper panel). The total RC as a function of the proton-beam energy E for different recoil-electron energies ε_2 and different values of the parameter ΔE: $\Delta E = 50$ keV (solid line), $\Delta E = 100$ keV (dashed line) (lower panel)

$$G_M(q^2) = G_M(0)\left(1 + \frac{1}{6}\, q^2\, \langle r_m^2 \rangle\right).$$

The values for $\langle r^2 \rangle$, $\langle r^4 \rangle$, and $\langle r_m^2 \rangle$ can be obtained, for example, from the recent analysis of the Mainz data [16], where the parametrizations for G_E and G_M are presented.

The dependences of the differential cross-section on the proton beam energy E for different values of the electron scattering angle θ_e are shown in Fig. 1. The cross-section has a minimum, which shifts to the smaller values of the proton beam energy, as the electron scattering angle increases, and, at this time, the magnitude of the cross-section becomes larger. It is due to the fact that the value of q^2 tends to zero, as the angle θ_e approaches the value 90^0. In this figure, we show also the effect of the inclusion of RCs. One can see that RCs are negative and increase with the proton beam energy.

In Fig. 2, we show the quantity $(1 - R)$, where $R = d\sigma_e/d\sigma_\mu$ is the ratio of the differential cross-

sections calculated with PCR determined from the electron [3] (muon [2]) experiments. One can see that the difference between the differential cross-sections $d\sigma_e$ and $d\sigma_\mu$ increases, as the angle θ_e decreases, and the proton beam energy becomes larger.

The upper panel of Fig. 3 shows the differential cross-section as a function of the proton-beam energy E for different recoil-electron energies ε_2: 10 MeV and 100 MeV. Increasing the energy ε_2 leads to decreasing the differential cross-section, since the value of q^2 becomes larger in this case. The lower panel of Fig. 3 shows the dependence of the total RC $(1+\delta)$ on the proton-beam energy E for different recoil-electron energies ε_2 and different values of the parameter ΔE: $\Delta E = 50$ keV (solid line), $\Delta E = 100$ keV (dashed line). All calculations are performed with PCR extracted from electron experiments.

In summary, the model-independent QED RCs to the differential cross-section of the elastic scattering of the proton beam on electrons at rest have been calculated. Under the kinematical conditions considered, the electric contribution to the cross-section dominates, and the magnetic contribution can be safely neglected. This allows a precise measurement of PCR.

This work was partially supported by the Ministry of Education and Science of Ukraine (project No. 0115U000474).

1. R. Pohl *et al.* The size of the proton. *Nature* **466**, 213 (2010) [DOI: 10.1038/nature09250].
2. A. Antognini *et al.* Proton structure from the measurement of 2S-2P transition frequencies of muonic hydrogen. *Science* **339**, 417 (2013) [DOI: 10.1126/science.1230016].
3. P.J. Mohr, B.N. Taylor, D.B. Newell. CODATA recommended values of the fundamental physical constants: 2010. *Rev. Mod. Phys.* **84**, 1527 (2012) [DOI: 10.1103/RevModPhys.84.1527].
4. X. Zhan *et al.* High-precision measurement of the proton elastic form factor ratio $\mu_p G_E/G_M$ at low Q^2. *Phys. Lett. B* **705**, 59 (2011) [DOI: 10.1016/j.physletb.2011.10.002].
5. J.C. Bernauer *et al.* High-precision determination of the electric and magnetic form factors of the proton. *Phys. Rev. Lett.* **105**, 242001 (2010) [DOI: 10.1103/PhysRevLett.105.242001].
6. A. Antognini *et al.* The proton radius puzzle. *J. Phys. Conf. Ser.* **312**, 032002 (2011) [DOI: 10.1088/1742-6596/312/3/032002].
7. M.M. Giannini, E. Santopinto. On the proton radius problem. arXiv:1311.0319v1 [hep-ph] (2013).
8. E. Kraus *et al.* Polynomial fits and the proton radius puzzle. *Phys. Rev. C* **90**, 045206 (2014) [DOI: 10.1103/PhysRevC.90.045206]; arXiv:1405.4735v1 [nucl-ex] (2014).
9. I.T. Lorenz, H.W. Hammer, Ulf-G. Meißner. The size of the proton: Closing in on the radius puzzle. *Eur. Phys. J. A* **48**, 151 (2012) [DOI: 10.1140/epja/i2012-12151-1]; arXiv:1205.6628v1 [hep-ph] (2012).
10. I.T. Lorenz, Ulf-G. Meißner. Reduction of the proton radius discrepancy by 3σ. *Phys. Lett. B* **737**, 57 (2014) [DOI: 10.1016/j.physletb.2014.08.010]; arXiv:1406.2962v1 [hep-ph] (2014).
11. K. Griffioen, C. Carlson, S. Maddox. Are electron scattering data consistent with a small proton radius? *Phys. Rev. C* **93**, 065207 (2016) [DOI: 10.1103/PhysRevC.93.065207]; arXiv:1509.06676v1 [nucl-ex] (2015).
12. M.O. Distler, T. Walcher, J.C. Bernauer. Solution of the proton radius puzzle? Low momentum transfer electron scattering data are not enough. arXiv:1511.00479v1 [nucl-ex] (2015).
13. M. Horbatsch, E.A. Hessels. Evaluation of the strength of electron-proton scattering data for determining the proton charge radius. *Phys. Rev. C* **93**, 015204 (2016) [DOI: 10.1103/PhysRevC.93.015204].
14. L.T. Lorenz, Ulf-G. Meißner, H.-W. Hammer, Y.-B. Dong. Theoretical constraints and systematic effects in the determination of the proton form factors. *Phys. Rev. D* **91**, 014023 (2015) [DOI: 10.1103/PhysRevD.91.014023].
15. K.M. Graczyk, C. Juszczak. Proton radius from Bayesian inference. *Phys. Rev. C* **90**, 054334 (2014) [DOI: 10.1103/PhysRevC.90.054334].
16. G. Lee, J.R. Arrington, R.J. Hill. Extraction of the proton radius from electron-proton scattering data. *Phys. Rev. D* **92**, 013013 (2015) [DOI: 10.1103/PhysRevD.92.013013].
17. V. Punjabi *et al.* The structure of the nucleon: Elastic electromagnetic form factors. *Eur. Phys. J. A* **51**, 79 (2015) [DOI: 10.1140/epja/i2015-15079-x].
18. D. Tucker-Smith, I. Yavin. Muonic hydrogen and MeV forces. *Phys. Rev. D* **83**, 101702 (2011) [DOI: 10.1103/PhysRevD.83.101702].
19. B. Batell, D. McKeen, M. Pospelov. New parity-violating muonic forces and the proton charge radius. *Phys. Rev. Lett.* **107**, 011803 (2011) [DOI: 10.1103/PhysRevLett.107.011803].
20. J.C. Bernauer. Proton Charge Radius and Precision Tests of QED. arXiv:1411.3743v1 [nucl-ex] (2014).
21. G.T. Adylov *et al.* The pion radius. *Phys. Lett. B* **51**, 402 (1974) [DOI: 10.1016/0370-2693(74)90239-1]; A measurement of the electromagnetic size of the pion from direct elastic pion scattering data at 50 GeV/c. *Nucl. Phys. B* **128**, 461 (1977) [DOI: 10.1016/0550-3213(77)90056-6].
22. E.B. Dally *et al.* Direct measurement of the π^- form factor. *Phys. Rev. Lett.* **39**, 1176 (1977) [DOI: 10.1103/PhysRevLett.39.1176]; Measurement of the π^- form factor.

Phys. Rev. D **24**, 1718 (1981) [DOI: 10.1103/PhysRevD.24.1718].

23. E.B. Dally *et al.* Elastic-scattering measurement of the negative-pion radius. *Phys. Rev. Lett.* **48**, 375 (1982) [DOI: 10.1103/PhysRevLett.48.375].
24. E.B. Dally *et al.* Direct measurement of the negative-kaon form factor. *Phys. Rev. Lett.* **45**, 232 (1980) [DOI: 10.1103/PhysRevLett.45.232].
25. D.Yu. Bardin, V.B. Semikoz, N.M. Shumeiko. Radiation corrections to pi-e scattering (in Russian). *Yad. Fiz.* **10**, 1020 (1969).
26. G.I. Gakh, A. Dbeyssi, E. Tomasi-Gustafsson, D. Marchand, V.V. Bytev. Proton-electron elastic scattering and the proton charge radius. *Phys. Part. Nuclei Lett.* **10**, 393 (2013) [DOI: 10.1134/S1547477113050099].
27. G.I. Gakh, A. Dbeyssi, D. Marchand, E. Tomasi-Gustafsson, V.V. Bytev. Polarization effects in elastic proton-electron scattering. *Phys. Rev. C* **84**, 015212 (2011) [DOI: 10.1103/PhysRevC.84.015212].
28. G. 't Hooft, M. Veltman. Scalar one-loop integrals. *Nucl. Phys. B* **153**, 365 (1979) [DOI: 10.1016/0550-3213(79)90605-9].
29. E.A. Kuraev, V.S. Fadin. On radiative corrections to $e^+ e^-$ single photon annihilation at high-energy. *Yad. Fiz.* **41**, 733 (1985) (in Russian); *Sov. J. Nucl. Phys.* **41** 466 (1985).

Received 07.06.16

Г.І. Гах, М.І. Кончатний, М.П. Меренков

МОДЕЛЬНО НЕЗАЛЕЖНІ
РАДІАЦІЙНІ ПОПРАВКИ В ПРУЖНОМУ
ПРОТОН-ЕЛЕКТРОННОМУ РОЗСІЯННІ

Р е з ю м е

Модельно незалежні КЕД радіаційні поправки обчислені для диференціального перерізу пружного розсіяння протонного пучка на електроні в стані спокою. Враховані радіаційні поправки зумовлені поляризацією вакуума та випромінюванням віртуального та м'якого фотонів в електронній вершині. Отримано числові оцінки цих поправок.